International Journal of Applied Science and Engineering

Prediction of residual strength of sustainable self-consolidating concrete exposed to elevated temperature using artificial intelligent technique

Faiq M. S. Al-Zwainy[1*], Shakir A. Salih[2], Mohammed R. Aldikheeli[3]

[1] *Department of Civil Engineering, Al-Nahrain University, Baghdad, Iraq*
[2] *Department of Civil Engineering, University of Technology, Baghdad, Iraq*
[3] *Department of Civil Engineering, Al-Kufa University, Baghdad, Iraq*

ABSTRACT

Self-consolidating concrete (SCC) is a very significant advance in concrete technology and became widely spread so it may be involuntary or accidently exposed to elevated temperature. Artificial intelligent techniques and especially artificial neural networks (ANNs) had proved its efficiency to solve complex systems such as concrete exposed to elevated temperature that are hard to model using usual modelling techniques such as mathematical modelling. The purpose of this study is to present an ANN model to predict the residual strength of sustainable (SCC) exposed to elevated temperature and to investigate which of the input variable has the most important impact on the model by conducting the sensitivity analysis. The results are indicated that the back propagation network with one hidden layer comprise two hidden nodes can be effectively used to predict the residual strength with R^2, MAPE% and AA% found to be 96.73%, 12.82% and 87.18% respectively. By using Garson algorithm method, the results are showed that fly ash content has the highest relative importance index% (R.I.I) and it was 24.6%.

Keywords: Sustainable, Self-consolidating concrete (SCC), Artificial intelligent techniques, Artificial neural networks (ANNs), Sensitivity analysis.

OPEN ACCESS

Received: April 13, 2018
Revised: November 10, 2020
Accepted: February 22, 2021

Corresponding Author:
Faiq M. S. Al-Zwainy
faiq.al-zwainy@eng.nahrainuniv.edu.iq

Publisher:
Chaoyang University of Technology
ISSN: 1727-2394 (Print)
ISSN: 1727-7841 (Online)

1. INTRODUCTION

Self-consolidating concrete is highly flowable, non-segregating concrete that can spread into place, fill in the formwork and encapsulate the reinforcement without any mechanical consolidation. Self-consolidating concrete (SCC) is a new generation concrete that consolidates without any external effort. Due to its advantages over the conventional concrete, the usage of SCC increases day by day. Understanding the behaviour of SCC is important in the design of structures subjected to elevated temperature. Self-compacting concrete (SCC) is being used in high-rise buildings and industrial structures which may be subjected to high temperatures during operation or in case of an accidental fire. Therefore the proper understanding of the effects of elevated temperatures on the properties of SCC is necessary (ACI 237R, 2007).

To produce this type of concrete high volume cement past is required, so high cement content is wanted (450–600 kg/m^3) (Gao et al., 2012; Dehwah, 2012) which is not desired neither technically nor economically/environmentally. The hope is to make the construction industry proceed toward the sustainability concept and to satisfy this hope the substituting additives such as filling materials and mineral admixtures can be used, especially in SCC (Domone, 2006). The study of "green", "sustainable" or "eco-efficient" concrete has advanced rising attention among the major contemporary publications about concrete because the affairs concerning the industrial wastes recycling, durability of concrete, environment and the cost will place a pressure on the employment of waste materials (Kraus et al., 2009). So in the current study, sustainable SCC was studied by

using the green materials: Portland limestone cement (PLC), high volume class F fly ash (HVFA) and Iraqi available cement kiln dust (CKD). One of the typical problems that may face the civil engineering is the analysis of the behaviour of concrete subjected to elevated temperature. Where estimation the residual strength of concrete that may exposed to elevated temperature before it facing such situations will be very important in rescue human life and the property. This complicated problem, because it has a large number of controlling parameters, may be solved by using the artificial neural network (ANN). This intelligent technique had proved its efficiency to solve complex systems and some recent researches proved that as follow:

- Eskandari and Ramin (2017), presented an artificial neural network (ANN) to predict the compressive strength of mortar mixtures containing different cement strength classes of CME 32.5, 42.5, and 52.5 MPa. In their study, a total of 810 specimens of 50-mm cubes were constructed in order to implementing the compressive strength test. After training the 17 neural networks with various numbers of hidden neurons and also two different nonlinear input activation functions as Tanh and Logistic, the ANN 5-11-1 network with Logistic function was chosen. Good agreement between predicted and experimental data was observed.
- Chithra et al. (2016), constructed three models for multiple regression analysis (MRA) and three others for ANN to predict the compressive strength of high performance concrete containing nano silica and copper slag as partial cement and fine aggregate replacement respectively. Artificial neural network models demonstrated more accuracy and had higher correlation than MRA models where the coefficient of determination (R^2) was 63.74%, 66.86% and 67.17% for MRA1, MRA2 and MRA3 respectively while it was 99.46%, 99.75% and 99.51% for ANN1, ANN2 and ANN3 respectively.
- Mashhadban et al. (2016), used PSOA (particle swarm optimization algorithm) and ANN to predict mechanical properties of fiber reinforced self-compacting concrete. They conclude that ANN is a flexible and accurate method in prediction of mechanical properties of fiber reinforced SCC properties. The coefficient of determination (R2) obtained by PSOA integrated with the ANN was 99.9%.
- Wang et al. (2015), used ANN and fuzzy inference system model (FIS) for predicting the free expansion strain of Self-stressing concrete (SSC) under wet curing conditions. To construct these models, 730 experimental data were gathered. The data used in the ANN and FIS models are arranged in a format of four input parameters that cover the water/cement ratio, cement abundance coefficient, cross-section area of specimens and curing time, and output parameter, which is the free expansion strain of SSC. The results of the analyses indicate that after successful learning the ANN model and FIS model have good performance in desirable accuracy and applicability.
- Ghafoori et al. (2013), studied several linear and nonlinear regressions and neural network models to estimate rapid chloride permeability of self - consolidating concrete. These prediction models were developed for different number of independent variables and for selecting testing and training samples two different strategies were adopted. The results of their study showed the superior performance of neural network models in comparison with the prediction models obtained by linear and nonlinear regressions, particularly when testing evaluations were chosen from the boundaries of mixture proportions where the correlation factor (CF) was found to be 99.8%.
- Parhi and Dash (2011), analyzed the dynamic behavior of a beam structure containing multiple transverse cracks using neural network. Results from neural network have been presented for comparison with the output from theoretical, finite-element, and experimental analysis. From the evaluation of the performance of the neural network it was observed that the developed method can be used as a crack diagnostic tool in the domain of dynamically vibrating structures.
- Rahman et al. (2010), outlined the application of the multi-layer perceptron ANN, ordinary kriging (OK), and inverse distance weighting (IDW) models in the estimation of local scour depth around bridge piers. It was shown that the artificial neural network model predicts local scour depth more accurately than the kriging and inverse distance weighting models. It was found that the ANN with two hidden layers was the optimum model to predict local scour depth.

2. EXPERIMENTAL WORK

2.1 Materials Characteristics

2.1.1 Cement

In the present study the cement used was local Portland-lime stone cement (PLC) available in the markets, Karasta CEM II/A-L 42.5 R. It complies with European Standard EN 197-1 (2000) and Iraqi industrial license No: 3868. The physical and chemical characteristics of cement used in this study are presented in Table 1.

2.1.2 Aggregates

As fine aggregate natural sand was used in this work. The grading, physical and chemical properties of the sand used are shown in Table 2. It has a fineness modulus of 2.5 and within the grading zone 3. A crushed gravel with a maximum size of 20 mm was used as a coarse aggregate, the grading, physical and chemical properties of gavel used are shown in Table 3. Both types of aggregate were conformed to the Iraqi specification No.45 / 1984.

Table 1. Chemical and physical characteristics of Portland limestone cement (PLC) used [a]

Oxides or property	PLC test results	Requirement of EN 197-1 (2000)	Requirement of Iraqi industrial license No: 3868 [b]
SiO_2	18.8	-	-
Al_2O_3	4.8	-	-
Fe_2O_3	2.7	-	-
CaO	61.9	-	-
MgO	2.5	-	≤ 5.0%
SO_3	2.6	≤ 4.0%	≤ 2.5% if C_3A less than 5% ≤ 2.8% if C_3A more than 5%
Na_2O	0.2	-	-
K_2O	1.1	-	-
$(Na_2O)_{eq.}$ [c]	0.92	-	-
L.O.I (Loss on Ignition)	4.5	-	-
Fineness (m^2/Kg)	390	-	-
Initial setting time (min.)	128	≥ 60.0	≥ 45.0
Final setting time (hr.)	3.3	-	-
2 days compressive strength (MPa)	23	≥ 20.0	≥ 20.0
28 days compressive strength (MPa)	49	≥ 42.5	≥ 42.5

[a] Chemical analysis and physical properties were carried out in the laboratory of Al – Kufa cement mill.
[b] Limit by ICOSQC (Iraqi central organization for standardization & quality control).
[c] $(Na_2O)_{eq.} = Na_2O+0.658\ K_2O$.

Table 2. Grading and some physical and chemical properties of sand used

Sieve size (mm)	Cumulative passing %	Limits of Iraqi specification No.45/1984, zone 3
4.75	97	90-100
2.36	89	85-100
1.18	75	75-100
0.60	60	60-79
0.30	22	12-40
0.15	5	0-10
Property	Test results	
Specific gravity	2.58	-
Sulfate content (SO_3) %	0.21	≤ 0.5
Absorption %	1.82	-
Materials finer than sieve No. 200	1.4	≤ 5.0
Fineness modulus	2.5	-

Table 3. Grading and some physical and chemical properties of gravel used

Sieve size (mm)	Cumulative passing%	Limits of Iraqi specification No. 45/1984
37.5	100	100
20	100	95-100
10	39	30-60
5	3	0-10
Property	Test results	
Specific gravity	2.62	-
Sulfate content (SO_3) %	0.03	≤ 0.1
Absorption %	0.7	-

2.1.3 Chemical Admixture

A high performance superplasticizer based on modified polycarboxylic ether which is commercially famous (GLENIUM 54) was used, for the liquefaction of the concrete mixtures to achieve the desired workability, throughout this study as a "high range water reducing admixture" (HRWRA). It complies with ASTM C494 (2005).

Table 4. Chemical analysis and physical properties of the fly ash and cement kiln dust [a]

Oxides or property	Fly ash	Cement kiln dust	ASTM C618-05 (2005) Class F requirement
SiO_2	50.5	16.7	$SiO_2 + Al_2O_3 + Fe_2O_3 > 70$
Al_2O_3	22.7	4.5	
Fe_2O_3	9.3	2.0	
CaO	10.8	44.5	
MgO	1.2	1.3	-
Na_2O	1.0	0.3	-
K_2O	0.8	3.7	-
TiO_2	0.7	-	-
SO_3	1.5	5.5	5.0 max.
Loss on ignition	1.2	20.0	6.0 max.
Specific gravity	2.12	-	-
Specific surface area (m^2/kg)	420	565	-

[a] Chemical analysis and physical properties were carried out in the laboratory of Al – Kufa cement mill.

Table 5. Characteristics of polypropylene fibres used*

Property	Values
Specific gravity	0.91g/cm³
Melting point	160 °C
Fibre diameter	18 µm
Fibre length	12 mm
Colour	White
Addition rate	0.6 kg/m³
Tensile strength	320-400 MPa

*According to manufacturer (Basf Chemical Company).

2.1.4 Fly Ash

Fly ash used in present study was obtained from Turkey. The physical and chemical properties of fly ash are tabulated in Table 4. It can be seen from Table 4 that the fly ash used is considered as class F fly ash as per ASTM C618 standard (2005).

2.1.5 Cement Kiln Dust

Cement kiln dust (CKD) is a by-product of cement production. Table 4 indicates the chemical composition and Fig. 1 shows the scanning electron microscopy (SEM) of the cement kiln dust used in this research. SEM is a type of electron microscope that produces images of a sample by scanning the surface with a focused beam of electrons. The electrons interact with atoms in the sample, producing various signals that contain information about the surface topography and composition of the sample.

2.1.6 Polypropylene Fibre

Monofilament polypropylene fibres were used in this work. It was provided from market and it is commercially known "RHEOFIBRE". Table 5 shows its characteristics.

2.2 Specimens Production and Heating and Cooling Procedure

Fourteen different SCC mixes were investigated in this study seven without and seven with polypropylene fibre. Table 6 shows the mixture proportions of these mixes. After appropriate mixing procedure that recommended by Long et al. (2014), Thanh and Ludwig (2015), all concrete mixes were casted in the 10 cm cubic moulds without any vibration and instantaneously covered with plastic wrap and kept

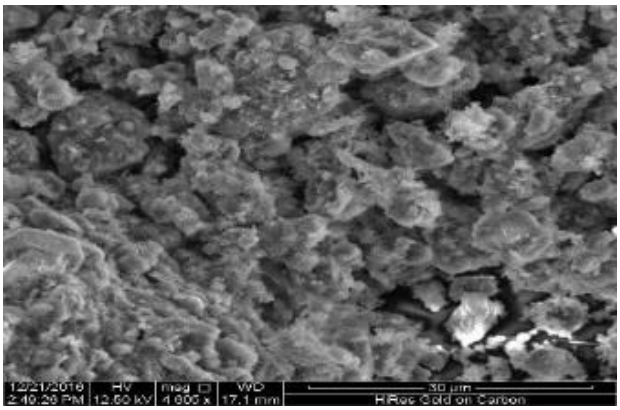

Fig. 1. SEM for CKD used

undisturbed for 24 hr. in laboratory circumstances. After 24 hr., specimens were removed from the moulds and placed in curing tank until 28 day then the specimens were placed in lab conditions until the age of 91 day. At the age of 91 day, specimens were placed in the manufactured electrical furnace which has a capacity of 1200°C (the temperature inside the furnace was at the room temperature at the time of putting the specimens) then heat was applied at a rate of 5°C /min until the desired temperature was reached. In

Table 6. Mix proportions of the concrete mixes

Mix ID	Mixture proportions (kg/m^3)							
	Cement	Fly ash	Cement kiln dust	Water	Sand	Gravel	W/P [a]	SP [b]
REF	500	-	-	180	800	800	0.36	0.8
40FA	300	200	-	180	800	800	0.36	0.7
50FA	250	250	-	180	800	800	0.36	0.6
60FA	200	300	-	180	800	800	0.36	0.55
20CKD	400	-	100	180	800	800	0.36	0.9
30CKD	350	-	150	180	800	800	0.36	1.1
50B	250	150	100	180	800	800	0.36	0.9

[a] W/P : water / powder : water / (cement + FA +CKD)

[b] SP : superplasticizer : (Lit/100Kg cementitious material)

addition to room temperature four temperature degrees were investigated (200°C, 400°C, 600°C and 800°C). After reaching the target temperature, the specimens were remained at this temperature for two hours as shown in Fig. 2. To ensure that the specimens were reached to the maximum temperature two type "K" thermocouples were placed at the surface of the specimens and the temperature was read by using a digital "ELE" thermometer as shown in Fig. 3. For cooling the specimens two techniques were adopted in the present study and they were slow cooling (in air) and rapid cooling (in water). The compressive strength test was performed according to the BS EN 12390-3:2002, by using ELE digital compression machine of 2000 KN. The number of the specimens produced was 126 (14 × 4 × 2) + (14 × 1) as shown in appendix (A) and each number represents the average of three specimens.

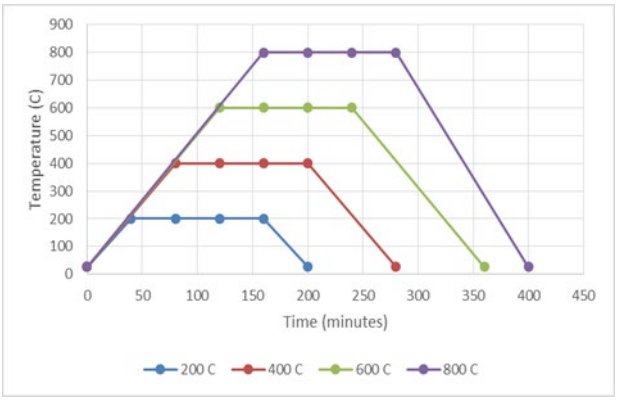

Fig. 2. Heating cycles imposed

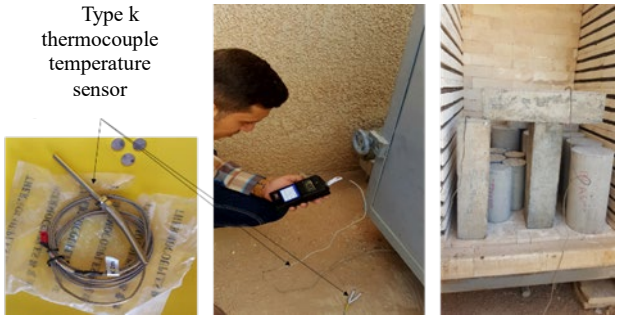

Fig. 3. Measuring the specimen temperature by using ELE thermometer

3. CONSTRUCTION THE PREDICTION MODEL

There are many applications that support the adoption of neural networks such as MATLAB, SPSS, Pythia and NeuroSolutions. In this study Neuframe Version 4 software was used to build the model because Neuframe is the leading neural networks simulation environment and it offers object oriented and soft to usage approach to solve problems using intelligent tools (Alzwainy et al., 2015). Fig. 4 shows the general components of Neuframe 4 software which is assembled to find the connection amongst the independent variables (inputs) and the dependent variables (output). The methodology for developing the prediction model by Neuframe 4 program has five phases as described below (Alzwainy, 2008):

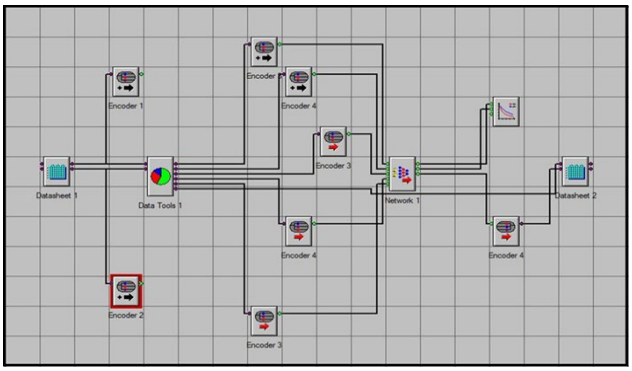

Fig. 4. Typical objects of NEUFRAME 4 software

3.1 Model Inputs and Outputs

The first step is to identify the input data and the output data and classified them whether it is quantity data or quality data. In this study seven independent variables were considered as input layer and one dependent variable which represents the output layer as shown in Fig. 5 and Table 7. The Neuframe 4 software equips Microsoft Excel sheet as shown in Fig. 4 (Datasheet1) which will contain the input and output data.

Table 7. Description of models factors

Type of variables	Code	Variables	Unit	Class of data
Independent variables	V1	Cement content	Kg/m^3	Quantity data
	V2	Superplasticizer content	Lit/100 Kg cementitious materials	Quantity data
	V3	Fly ash content	Kg/m^3	Quantity data
	V4	Cement Kiln Dust content	Kg/m^3	Quantity data
	V5	Type of cooling	Water cooling = 0 Air cooling = 1	Quality data
	V6	Polypropylene fibres	Without fibre = 2 With fibre = 3	Quality data
	V7	Temperature degree	Celsius	Quantity data
Dependent variable	Y	Compressive strength	MPa	Quantity data

Table 8. Effect of data division on performance of ANN model

Data division %			Training error%	Testing error%	Correlation (R)%	(R^2) %
training	testing	querying				
80	10	10	7.41	14.83	95.31	90.85
80	5	15	6.25	16.47	84.55	71.5
80	15	5	6.68	17.69	96.03	92.23
77	10	13	6.98	17.06	92.29	85.18
77	13	10	7.04	17.14	95.55	91.30
77	15	8	5.93	18.15	84.94	72.15
75	15	10	6.72	16.12	94.79	89.86
75	10	15	6.59	14.49	84.22	70.94
75	20	5	6.59	13.67	78.06	60.93
75	5	20	6.83	17.30	87.76	77.02
72	20	8	6.91	14.06	85.23	72.64
70	20	10	6.87	13.75	95.15	90.54
70	10	20	6.87	17.04	87.66	76.85
70	15	15	6.00	14.13	84.86	73.02
70	18	12	6.83	16.99	92.35	85.29
70	22	8	6.84	17.24	85.84	73.69
69	21	10	7.03	15.16	95.07	90.4
68	20	12	7.25	14.54	95.1	90.44
68	18	14	6.99	15.48	86.10	74.13
68	22	10	7.46	17.12	92.09	84.81

Table 9. Effect of distribution method on the performance of ANN

Data division %			Division type	Training error %	Testing error %	R%	R^2%
Training	Testing	Querying					
70	20	10	Blocked	6.94	13.51	94.24	88.82
70	20	10	Striped	6.87	13.75	95.15	90.54
70	20	10	Random	6.74	17.54	81.o2	65.64

3.2 Pre-processing and Data Partition

For effective utilize from artificial neural system it is very important to split the information into three groups: training group where the learning is done on this set of data and it is used to determine the weights. The second group is the testing group where this set of data is utilized for assessing the generalization capability of the grid and assessing the execution of the network, and the testing error which is very important. The latest group is the validation group and this set of data is used for generalization to make the best output for unknown examples. In the present study, by using the data tools1 as shown in Fig. 4 and depend on the lowest testing error which is 13.75% and the maximum correlation coefficient (R) which is 95.15% the top data partition is 70% for training group, 20% for testing group and 10% for validation group as tabulated in Table 8. Thus, this division was selected in building the model. By using the same object (the data tools1) as shown in Fig. 4 there are three distribution types (Blocked, Striped and Random) and it is important to choice the best distribution and it was "Striped" as tabulated in Table 9.

3.3 Scaling of Data

Before the data are supplied to the network it is significant to preprocess the data in an appropriate formula and this done as soon as the existing data had been allocated into their subsets (i.e. training, testing and validation). This operation is required to guarantee that all inputs take the same concern through the training course. Additionally, pre-processing generally accelerates the training process. Transformation, data scaling and normalization are different methods for preprocessing. As the boundaries of the activation functions used in the hidden stratum and output stratum ranged between (-1) to (1) for the tanh activation function as in Equation (1) and between (0) to (1) for the sigmoid activation function as in Equation (2) so it is important to scale the output data, to be adequate with these boundaries (Shahin et al., 2002).

$$Scaled\ value\ (Z_n)\ Tanh = (2 * (Z - Z_{min}) / (Z_{max} - Z_{min}) - 1 \quad (1)$$

$$Scaled\ value\ (Z_n)\ Sigmoid = (Z - Z_{min}) / (Z_{max} - Z_{min}) \quad (2)$$

Where Z is the original value.

3.4 Model Performance

3.4.1 Model Architecture

There are two types of learning; these are supervised and unsupervised learning. The supervised learning network is used in current study, because it has the input data with the related needed output data so the net can teach to estimate the connection amongst two variables by training. Chosen the optimal number of the stratums and the number of the processing elements in every layer is very important stage in building the model. Generally, in any neural network there are always one layer represents the input variables and one layer represents the output variables. The number of model inputs and outputs controlled the number of processing elements in the input and output stratums respectively (Shahin et al., 2002). For determining best ANN architecture, no united philosophy is found. In this study a trial-and-error method were utilized to find the number of the hidden stratums and the number of its nodes and it was found that one hidden layer was the best and beginning with one hidden neuron and then increasing the quantity of the neurons as shown in Table 10. The network with two hidden nodes has the lowest training and testing errors and they were 5.03% and 13.49% respectively and the highest correlation coefficient (R) was 98.72%. So the optimal architecture for the network is shown in Fig. 5.

3.4.2 Activation (transfer) Function

In neural networks, the transfer function (may be linear or nonlinear) is the function which designates the output behaviour of a node. There are three main kinds of activation functions can be utilized to convert input signal into output and these are linear function, sigmoid function and hyperbolic tangent function. In this study the effect of using various activation function was investigated as shown in Table 11. It is clearly form this table that the top action of the network attained when using the sigmoid transfer function in both hidden and output layers where it has the lowest training and testing error and they were 5.03% and 13.49% respectively and the highest correlation coefficient (R) was 98.72%.

3.4.3 Training (learning) of the Network

The purpose of training the network is to aid it to generalize future data and produce the most perfect answers. By adjusting the connection weights the system will learn new knowledge where changing the mass of every connection will make the net offers an enhanced estimation of the preferred output. The learning capability of a neural network is controlled by the algorithmic method selected for training and by its architecture (Haykin, 2001). There are many types of algorithms used in the training process but the most popular one is the back propagation algorithm (BP) which was adopted in the current study. The influence of the internal factors (momentum term and learning rate) that governing the back propagation algorithm on the action of the two hidden layer nodes model was studied in current work and it is shown in Table 12 and Table 13 respectively.

From these tables it is clearly that the best momentum term and learning rate were 0.8 and 0.2 respectively, since they provided the best performance of the network where the testing error was the lowest (13.49) and the correlation coefficient (R) was the highest (98.72%). So these parameters were used in building the model.

Table 10. Effect of hidden layer nodes number on the performance of ANN

No. of nodes	Training error %	Testing error %	R%	R^2%
1	6.87	13.75	95.15	90.54
2	5.03	13.49	98.72	97.46
3	5.54	12.9	96.57	93.26
4	5.14	13.01	98.38	96.78
5	5.79	13.88	97.7	95.46
6	5.13	13.40	98.09	96.22
7	5.36	21.63	97.40	94.87
8	5.32	15.84	98.10	96.25
9	5.33	19.33	97.44	94.96
10	5.29	14.74	97.25	94.58

Table 11. Impact of transfer function on the performance of ANN

Parameters effect	Transfer function		Training error %	Testing error %	R%	R^2%
	Hidden layer	Output layer				
Division selected (striped) No. of hidden layer nodes (2) Momentum rate (0.8) learning rate (0.2)	Sigmoid	Sigmoid	5.03	13.49	98.72	97.46
	Sigmoid	Tanh	52.32	52.87	16.46	2.71
	Tanh	Sigmoid	5.59	14.81	96.81	93.73
	Tanh	Tanh	52.32	33.80	63.67	40.54

Table 12. Impact of momentum term on the performance of ANN

Parameters effect	Momentum term	Training error %	Testing error %	R%	R^2%
Division selected (striped) No. of hidden layer nodes (2) learning rate (0.2) transfer function in the hidden layer (sigmoid) transfer function in the output layer (sigmoid)	0.7	5.28	13.49	98.71	97.44
	0.8	5.03	13.49	98.72	97.46
	0.85	4.90	13.49	98.69	97.40
	0.9	5.27	13.49	98.58	97.19
	0.95	5.24	13.49	97.84	95.74

Table 13. Impact of learning rate on the performance of ANN

Parameters effect	Learning rate	Training error %	Testing error %	R%	R^2%
Division selected (striped) No. of hidden layer nodes (2) Momentum rate (0.8) transfer function in the hidden layer (sigmoid) transfer function in the output layer (sigmoid)	0.05	5.47	13.01	98.68	97.38
	0.1	5.29	13.17	98.71	97.43
	0.15	5.35	13.33	98.70	97.42
	0.2	5.03	13.49	98.72	97.46
	0.25	5.22	13.65	98.71	97.43
	0.3	5.22	13.82	98.69	97.39
	0.4	5.55	14.18	98.65	97.32
	0.5	5.40	14.68	98.60	97.23
	0.6	5.77	15.31	98.59	97.21
	0.7	6.88	16.07	98.66	97.35
	0.8	5.89	16.98	98.65	97.32

Training of the network was ended when either the average error value fell below a pre-limited value (in this study 5% was selected) or the number of training epochs overstepped a pre-defined threshold (in this study 10000 epochs was selected). As soon as the training of the network is completed, it can be used to estimate the output for given set of input values.

3.5 ANN Model Equation

The connection weights amongst the input stratum nodes and the hidden stratum nodes in addition to the connection weights between the hidden stratum nodes and the output stratum node which were gained by the optimum network can be used to translate the network into a simple formula by the aid of the threshold or "bias" of the hidden and

output nodes. Fig. 5 and Table 14 show the connection weight and the threshold level of the network. Depending on sigmoid transfer function Equation (3) and the connection weights and bias from Table 14 the equation of compressive strength prediction can be expressed as follow:

$$f = {}^{1}/_{1 + exp^{-x}} \quad (3)$$

Where x is the weighted sum of the inputs from the previous layer to a specific node.

$$Y = \frac{1}{1+ e^{(1.857 \ + \ 4.478 \tanh(x_1) \ - \ 4.771 \ tanh \ (x_2)}} \quad (4)$$

Where:

$$X_1 = [(\theta_8) + (w_{8-1} * V_1) + (w_{8-2} * V_2) + (w_{8-3} * V_3) + (w_{8-4} * V_4) + (w_{8-5} * V_5) + (w_{8-6} * V_6) + (w_{8-7} * V_7)\ ] \quad (5)$$

$$X_2 = [(\theta_9) + (w_{9-1} * V_1) + (w_{9-2} * V_2) + (w_{9-3} * V_3) + (w_{9-4} * V_4) + (w_{9-5} * V_5) + (w_{9-6} * V_6) + (w_{9-7} * V_7)\ ] \quad (6)$$

So:

$$X_1 = [\ -1.046 + 0.325*V_1 - 0.083*V_2 - 2.395*V_3 + 1.733*V_4 - 0.141*V_5 - 0.379*V_6 + 0.316*V_7\ ] \quad (7)$$

$$X_2 = [\ -0.161 + 0.813*V_1 + 2.161*V_2 + 0.425*V_3 - 0.472*V_4 + 0.246*V_5 - 0.043*V_6 - 1.665*V_7\ ] \quad (8)$$

Here, it is necessary to take attention that all input variables (V_1, V_2, V_3, V_4, V_5, V_6, and V_7) in Equation (5) and Equation (6) had been transformed to standard values ranging between (0 and 1) as it is demanded by the Neuframe v.4 software. So in order to calculate the estimated value of the compressive strength in real value the input variables must be re-scaled by using Equation (2) and the training data minimum and range used in the ANN model. Lastly, the final form of the equation of the compressive strength estimation will be as follow:

$$Y = \frac{62}{1+ e^{(1.857 \ + \ 4.478 \tanh(x_1) \ - \ 4.771 \ tanh \ (x_2)}} + 13 \quad (9)$$

Where:

Y= estimated compressive strength (MPa)

$$X_1 = \{-0.4327 + 0.0011*V_1 - 0.151*V_2 - 0.008*V_3 + 0.0115*V_4 - 0.141*V_5 - 0.379*V_6 + 0.0004*V_7\} \quad (10)$$

$$X_2 = \{-2.72 + 0.0027*V_1 + 3.929*V_2 + 0.0014*V_3 - 0.0031*V_4 + 0.246*V_5 - 0.043*V_6 - 0.0022*V_7\} \quad (11)$$

For better clarifying the employment of the prediction equation, the following numerical example can be used: Data given: (V_1 = 350, V_2 = 1.1, V_3 = 0, V_4 = 150, V_5 = 1, V_6 = 3, and V_7 = 800). The predicted compressive strength value using Equation (9) will be 19.5 MPa. This predicted value show good comparison with actual value of measured compressive strength (17.0 MPa).

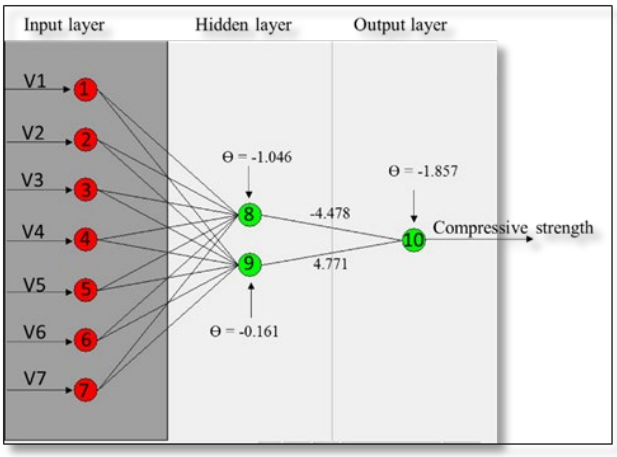

Fig. 5. Structure of the optimal ANN

Table 14. Weights and threshold (Θ) of the optimal ANN

Hidden layer node	W_{ji} (weight from node (i) in the input layer to node (j) in the hidden layer)				Hidden layer threshold (Θ_j)
J = 8	i = 1	i = 2	i = 3	i = 4	-1.046
	0.325	-0.083	-2.395	1.733	
	i = 5	i = 6	i = 7		
	-0.141	-0.379	0.316		
J = 9	i = 1	i = 2	i = 3	i = 4	-0.161
	0.813	2.161	0.425	-0.472	
	i = 5	i = 6	i = 7	-	
	0.246	-0.043	-1.665		
Output layer node	W_{ji} (weight from node (i) in the hidden layer to node (j) in the output layer)				Output layer threshold (Θ_j)
J = 10	i = 8	i = 9	-	-	-1.857
	-4.478	4.771	-	-	

Table 15. Verification of the model

Obs.	V1	V2	V3	V4	V5	V6	V7	Y actual	Y equation
1	250	0.6	250	0	1	3	600	45.8	48.1
2	200	0.55	300	0	0	3	400	43.5	44.5
3	350	1.1	0	150	1	2	400	25.0	35.4
4	300	0.7	200	0	0	3	800	32.6	36.4
5	250	0.6	250	0	1	2	200	68.5	74.4
6	400	0.9	0	100	1	2	800	18.3	14.5
7	350	1.1	0	150	0	3	600	21.9	23.2
8	300	0.7	200	0	1	3	200	71.6	75.0
9	350	1.1	0	150	0	2	400	23.6	26.9
10	500	0.8	0	0	0	2	800	33.6	38.8
11	250	0.6	250	0	0	2	600	37.2	37.6
12	200	0.55	300	0	1	3	200	64.8	72.2
13	300	0.7	200	0	0	2	800	30.5	37.5
the coefficient of correlation (R) = 98.35%									

4. MODEL VERIFICATION

There are many important statistical measures that may be applied to assess the performance and accuracy of the built model (Salah et al., 2019; Nidal et al., 2020; Ibraheem et al., 2020)

1. Mean percentage error (MPE): give an idea about the agreement between predicted and real values.

$$MPE = \left[\sum\left(\frac{A-E}{A}\right) / \ n\right] * 100 \ \% \quad (12)$$

2. Root mean squared error (RMSE)

$$RMSE = \sqrt{\frac{\sum(E-A)^2}{n}} \quad (13)$$

3. Mean absolute percentage error (MAPE)

$$MAPE = \left[\sum\left(\frac{|A-E|}{A}\right) * 100\%\right] \ / \ n \quad (14)$$

4. Average accuracy percentage (AA%): give the accuracy degree of the model.

$$AA\% = 100 - MAPE \quad (15)$$

5. The coefficient of correlation (R)
6. The coefficient of determination (R^2)

Where: A is the actual value, E is the estimated value and n is number of cases for validation.

The last two coefficients (R and R^2) were used to measure how well the model outputs match the real value (target) while RMSE and MAPE were used to measure the average error of the model. It can be seen from Table 15 and Fig. 6 that the estimated compressive strength has a very good correlate with the actual value and the coefficient of correlation (R) and the coefficient of determination (R^2) were 98.35% and 96.73% respectively.

According to the statistical measures that tabulated in Table 16 it can be seen that the mean absolute percentage error (MAPE) and average accuracy percentage (AA%) are found to be 12.82% and 87.18% respectively. So, it can be concluded that the built model has a good performance in compressive strength prediction.

Table 16. Statistical measures for model

Description	Result
MPE	-9.61
RMSE	5.08
MAPE	12.82
AA%	87.18
R	98.35
R^2	96.73

5. SENSITIVITY ANALYSIS OF THE ANN MODEL INPUTS

The ANN were used to develop the predictive model by feeding the input variables to the network and an output was estimated but there is an additional question that important to know. Which of the input variables have the most important influence on the predicted value (output)? The sensitivity analysis offers the answer for this question.

There are several techniques can be utilized to find the relative importance index of the input variables such as connection weights method, most squares method and Garson Algorithm method. In the present study Garson Algorithm method was used. It is important to know that in this method the absolute values of the final connection weights are used. The main steps of the Garson Algorithm method is as follow:

1. Prepare the final weights of the connections (amongst the input neurons and the hidden neurons) and (amongst the hidden neurons and the output neuron) from Table 14.
2. By multiplying the absolute value of the hidden-output linking weight by the absolute value of the hidden-input linking weight of all input variables find the product Pij for every hidden neuron, the result shown in below.

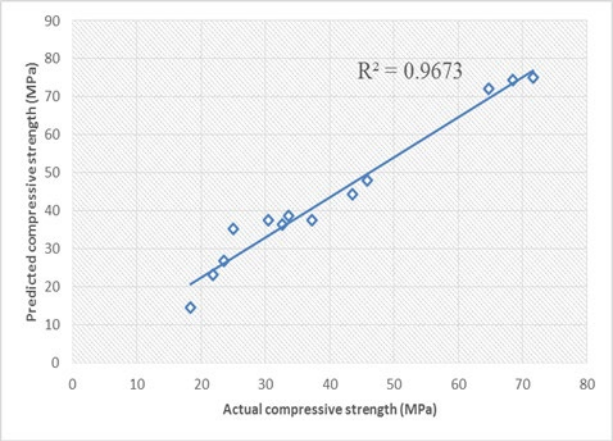

Fig. 6. Correlation between the actual and predicted compressive strength

J = 8	v = 1	v = 2	v = 3	v = 4	v = 5	v = 6	v = 7
	1.455	0.372	10.725	7.76	0.631	1.697	1.415
J = 9	v = 1	v = 2	v = 3	v = 4	v = 5	v = 6	v = 7
	3.879	10.31	2.028	2.252	1.174	0.205	7.944

3. Find Qij for each hidden node (by dividing Pij) for each variable by summation of Pij for all variables. The results as shown below:

J = 8	v = 1	v = 2	v = 3	v = 4	v = 5	v = 6	v = 7
	0.028	0.007	0.207	0.151	0.012	0.033	0.027
J = 9	v = 1	v = 2	v = 3	v = 4	v = 5	v = 6	v = 7
	0.075	0.199	0.039	0.043	0.023	0.004	0.153

4. Find Sj for each input node (by summation of the Qij) for the same input node). For example S1 = 0.028 + 0.075 = 0.103. The results as shown below:

v = 1	v = 2	v = 3	v = 4	v = 5	v = 6	v = 7
0.103	0.206	0.246	0.194	0.035	0.036	0.180

5. To get the relative importance index% (R.I.I) divided Sj for each input variable by the summation of all the input variables (here is equal to 1). The result will be as below:

	V1	V2	V3	V4	V5	V6	V7
R.I.I%	10.3	20.6	24.6	19.4	3.5	3.6	18
Rank	5	2	1	3	7	6	4

These results shown in Fig. 7 indicate that the variables (V3, V2, V4 and V7) have the most important influence on the predicted model with a relative importance index (24.6%, 20.6%, 19.4% and 18%) respectively.

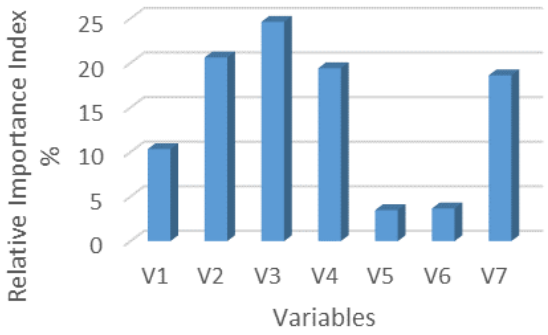

Fig. 7. Relative importance index % of the input variables

6. CONCLUSIONS

This study experimentally determined the residual compressive strength of sustainable self-consolidating concrete under elevated temperature. The experimental data are modelled through neural networks by Neuframe v.4 software and the following conclusion can be extracted:

- The optimum ANN is selected with 5.03% and 13.49% training and testing errors respectively and 98.72% correlation.
- The best data division is found to be 70% for training set, 20% for testing set and 10% for validation with striped data division. Back propagation algorithm is used in the learning process. Sigmoid transfer function is used in both hidden and output layers with two hidden neurons.
- The built model from ANN has a very good performance in compressive strength prediction as it has mean absolute percentage error (MAPE) and average accuracy percentage (AA%) of 12.82% and 87.18% respectively.
- The sensitivity analysis by using Garson Algorithm indicates that fly ash content has the highest relative importance index% and it was 24.6%.

REFERENCES

ACI 237R, 2007. Self-Consolidating concrete. American Concrete Institute 2007.

Alzwainy, F. 2008. The use of artificial neural network for estimating total cost of highway construction projects. Ph.D. dissertation. University of Baghdad.

Alzwainy, F., Mohammed, I., Mohsen, D. 2015. Earned value management in construction project. LAMBERT Academic Publishing. Germany.

ASTM C 494, 2005. Standard specification for chemical admixtures for concrete. American Society for Testing and Materials.

ASTM C 618, 2005. Standard specification for coal fly ash and raw calcined natural pozzolan for use in concrete. American Society for Testing and Materials.

BS EN 12390-3:2002. Testing hardened concrete part3: Compressive strength of test specimens. British Standard.

Chithra, S., Kumar, S., Chinnaraju, K., Ashmita, F. 2016. A comparative study on the compressive strength prediction models for High Performance Concrete containing nano silica and copper slag using regression analysis and Artificial Neural Networks. Construction and Building Material. 114, 528-535.

Dehwah, H. 2012. Mechanical properties of self-compacting concrete incorporating quarry dust powder, silica fume or fly ash. Construction and Building Material. 26, 547–551.

Domone, P. 2006. Self-compacting concrete: An analysis of 11 years of case studies. Cement and Concrete Composites. 28, 197–208.

EN 197-1, 2000. Cement - Part 1: Composition, Specifications and conformity criteria for common cements. European Standard.

Eskandari, H., Ramin, K. 2017. ANN prediction of cement mortar compressive strength, influence of cement strength class. Construction and Building Material. 138, 1–11.

Gao, X., Kawashima, S., Liu, X., Surendra, P. 2012. Influence of clays on the shrinkage and cracking tendency of SCC. Cement and Concrete Composites. 34, 478–485.

Ghafoori, N., Meysam, N., Sobhani, J., Mohammad, A. 2013. Predicting rapid chloride permeability of self-consolidating concrete: A comparative study on statistical and neural network models. Construction and Building Material. 44, 381–390.

Haykin, S. 2001. Neural networks: A comprehensive foundation. Second Edition, Pearson Education Inc., New Delhi, India.

Ibraheem, A., Duaa, A., Faiq, M. 2020. Predicting earned value indexes in residential complexes, Construction projects using artificial neural network model. International Journal of Intelligent Engineering and Systems. 13, 248–259.

Iraqi Specification, No.45/1984. Aggregates from natural sources for concrete and construction. National Center for Construction Laboratories and Researches.

Kraus, R., Naik, T., Ramme, B., Kumar, R. 2009. Use of foundry silica-dust in manufacturing economical self-consolidating concrete. Construction and Building Material. 23, 3439–3442.

Long, W., Khayat, K., Lemieux, G., Hwang, S., Han, N. 2014. Performance - Based specifications of workability characteristics of prestressed, Precast Self-Consolidating concrete - A North American prospective. MDPI, Material Journal. 7, 2474–2489.

Mashhadban, H., Kutanaei, S., Sayarinejad, M. 2016. Prediction and modeling of mechanical properties in fiber reinforced self-compacting concrete using particle swarm optimization algorithm and artificial neural network. Const and Build Mater. 119, 277–287.

Nidal, A., Shelan, M., Hadi, S., Faiq, M. 2020. Predicting index to complete schedule performance indicator in highway projects using artificial neural network model. Archives of Civil Engineering. 66, 541–554.

Parhi, D., Dash, A. 2011. Application of neural networks and finite elements for condition monitoring of structures. Proceedings of the Institution of Mechanical Engineers. 225, 1329–1339.

Rahman, H., Alireza, K., Reza, G. 2010. Application of artificial neural network, kriging, and inverse distance weighting models for estimation of scour depth around bridge pier with bed sill, Journal of Software Engineering and Applications. 3, 944–964. http://www.SciRP.org/journal/jsea

Salah, Kh. Z., Noora, S.F., Ibrahim, A.A., Faiq, M.S., Al-Zwainy, Mohammed, A.A., Ibraheem, A.M. 2019. Prediction of dust storms in construction projects using intelligent artificial neural network technology. Periodicals of Engineering and Natural Sciences. 7, 1659–1666.

Shahin, M., Jaska, M., Maier, H. 2002. Predicting settlement of shallow foundations using neural networks. Journal of Geotechnical and Geoenvironmental Engineering. 128, 785–793.

Thanh, H., Ludwig, H. 2015. Effect of rice husk ash and other mineral admixtures on properties of self-compacting high performance concrete. Materials and Design. 89, 156–166. http://dx.doi.org/10.1016/j.matdes.2015.09.120

Wang, B., Teng, M., Jin, H. 2015. Prediction of expansion behavior of self-stressing concrete by artificial neural networks and fuzzy inference systems. Construction and Building Material. 84, 184–191.

Appendix (A). Total laboratory data

No.	Actual data								Data partition
	Y	V1	V2	V3	V4	V5	V6	V7	
1	68.7	500	0.8	0	0	1	3	200	T
2	69.5	500	0.8	0	0	1	2	200	T
3	75.1	500	0.8	0	0	1	3	200	T
4	70.4	500	0.8	0	0	0	3	200	T
5	65	500	0.8	0	0	1	2	400	T
6	69.8	500	0.8	0	0	0	2	400	T
7	70.5	500	0.8	0	0	0	3	400	T

8	62.6	500	0.8	0	0	1	2	600	S
9	65.7	500	0.8	0	0	1	3	600	V
10	62.7	500	0.8	0	0	0	2	600	T
11	58.4	500	0.8	0	0	1	2	800	T
12	33.6	500	0.8	0	0	0	2	800	T
13	64.2	300	0.7	200	0	1	3	200	T
14	66.7	300	0.7	200	0	0	2	200	T
15	67.3	300	0.7	200	0	0	3	200	T
16	65.5	300	0.7	200	0	1	2	400	T
17	65.5	300	0.7	200	0	1	3	400	S
18	63.7	300	0.7	200	0	0	2	400	S
19	62.8	300	0.7	200	0	0	3	400	V
20	62.2	300	0.7	200	0	1	3	600	T
21	60.1	300	0.7	200	0	0	2	600	T
22	61.5	300	0.7	200	0	0	3	600	T
23	41.3	300	0.7	200	0	1	2	800	T
24	30.5	300	0.7	200	0	0	2	800	T
25	67.3	250	0.6	250	0	1	2	200	T
26	68.5	250	0.6	250	0	1	2	200	T
27	68.3	250	0.6	250	0	1	3	200	S
28	63.6	250	0.6	250	0	0	2	200	S
29	66.4	250	0.6	250	0	0	3	200	V
30	64.4	250	0.6	250	0	1	3	400	T
31	57.2	250	0.6	250	0	0	3	400	T
32	43.4	250	0.6	250	0	1	2	600	T
33	45.8	250	0.6	250	0	1	3	600	T
34	37.2	250	0.6	250	0	0	2	600	T
35	36.6	250	0.6	250	0	1	2	800	T
36	29.5	250	0.6	250	0	0	2	800	S
37	65.8	200	0.55	300	0	1	2	200	S
38	67.3	200	0.55	300	0	1	3	200	V
39	64.8	200	0.55	300	0	1	3	200	T
40	60.3	200	0.55	300	0	0	3	200	T
41	55.6	200	0.55	300	0	1	2	400	T
42	40.1	200	0.55	300	0	0	2	400	T
43	43.5	200	0.55	300	0	0	3	400	T
44	42.1	200	0.55	300	0	1	3	600	T
45	35.2	200	0.55	300	0	0	2	600	T
46	30.2	200	0.55	300	0	1	2	800	S
47	32.5	200	0.55	300	0	1	3	800	S
48	64.7	400	0.9	0	100	1	3	200	V
49	59.3	400	0.9	0	100	1	2	200	T
50	52.7	400	0.9	0	100	0	2	200	T
51	65.5	400	0.9	0	100	0	3	200	T
52	45.3	400	0.9	0	100	1	2	400	T
53	27.2	400	0.9	0	100	0	2	400	T
54	49.1	400	0.9	0	100	0	3	400	T
55	25.2	400	0.9	0	100	1	2	600	T
56	23.8	400	0.9	0	100	0	2	600	S
57	25.4	400	0.9	0	100	0	3	600	S
58	18.3	400	0.9	0	100	1	2	800	V
59	15.5	400	0.9	0	100	0	2	800	T
60	50.7	350	1.1	0	150	1	2	200	T
61	55.8	350	1.1	0	150	1	3	200	T
62	35.1	350	1.1	0	150	1	2	200	T
63	58.5	350	1.1	0	150	1	3	200	T
64	25	350	1.1	0	150	1	2	400	T

65	23.6	350	1.1	0	150	0	2	400	S
66	28.4	350	1.1	0	150	0	3	400	S
67	25.8	350	1.1	0	150	1	3	600	V
68	20.5	350	1.1	0	150	0	2	600	T
69	16.2	350	1.1	0	150	1	2	800	T
70	13.1	350	1.1	0	150	0	2	800	T
71	64.8	250	0.9	150	100	1	2	200	T
72	69	250	0.9	150	100	1	2	200	T
73	75.2	250	0.9	150	100	1	3	200	T
74	67.6	250	0.9	150	100	0	2	200	T
75	63.1	250	0.9	150	100	1	2	400	S
76	60.7	250	0.9	150	100	0	2	400	S
77	65.6	250	0.9	150	100	0	3	400	V
78	59.2	250	0.9	150	100	1	3	600	T
79	53.5	250	0.9	150	100	0	2	600	T
80	55.1	250	0.9	150	100	0	3	600	T
81	46.1	250	0.9	150	100	1	2	800	T
82	30.2	250	0.9	150	100	0	2	800	T
83	46.4	500	0.8	0	0	0	3	800	T
84	31.3	250	0.6	250	0	0	3	800	T
85	31.4	200	0.55	300	0	0	3	800	S
86	16.6	400	0.9	0	100	0	3	800	S
87	13.8	350	1.1	0	150	0	3	800	V
88	32.5	250	0.9	150	100	0	3	800	T
89	67.8	500	0.8	0	0	0	2	200	T
90	62.6	500	0.8	0	0	0	3	600	T
91	60.9	500	0.8	0	0	1	3	800	T
92	32.6	300	0.7	200	0	0	3	800	T
93	64.1	300	0.7	200	0	1	2	600	T
94	71.6	300	0.7	200	0	1	3	200	S
95	68.8	250	0.6	250	0	1	3	200	S
96	58.5	250	0.6	250	0	1	2	400	V
97	39.7	250	0.6	250	0	0	3	600	T
98	65.6	200	0.55	300	0	0	2	200	T
99	48.5	200	0.55	300	0	1	3	400	T
100	29.3	200	0.55	300	0	0	2	800	T
101	68.1	400	0.9	0	100	1	2	200	T
102	69.4	400	0.9	0	100	1	3	200	T
103	46.6	400	0.9	0	100	1	3	600	T
104	29.5	350	1.1	0	150	0	2	200	S
105	26.5	350	1.1	0	150	1	3	400	S
106	21.9	350	1.1	0	150	0	3	600	V
107	67.4	250	0.9	150	100	1	3	200	T
108	64.5	250	0.9	150	100	1	2	600	T
109	68.4	250	0.9	150	100	1	3	400	T
110	58.3	400	0.9	0	100	1	3	400	T
111	38.4	250	0.6	250	0	1	3	800	T
112	62.6	200	0.55	300	0	1	2	200	T
113	39.8	300	0.7	200	0	1	3	800	T
114	66.2	500	0.8	0	0	1	2	200	S
115	66	300	0.7	200	0	1	2	200	S
116	55.5	250	0.6	250	0	0	2	400	V
117	37.5	200	0.55	300	0	0	3	600	T
118	19.5	400	0.9	0	100	1	3	800	T
119	16.9	350	1.1	0	150	1	3	800	T
120	69.8	250	0.9	150	100	0	3	200	T
121	44.7	250	0.9	150	100	1	3	800	T

122	65.4	500	0.8	0	0	1	3	400	T
123	40	200	0.55	300	0	1	2	600	T
124	61.1	300	0.7	200	0	1	2	200	S
125	22.1	350	1.1	0	150	1	2	600	S
126	44.8	350	1.1	0	150	0	3	200	V

T = training, S = testing, V = validation